



Research paper

Discovery of novel small molecule inhibitors of lysine methyltransferase G9a and their mechanism in leukemia cell lines



Shukkoor M. Kondengaden ^{a,1}, Liu-fei Luo ^{b,1}, Kenneth Huang ^a, Mengyuan Zhu ^a, Lanlan Zang ^{a,c}, Eudoxie Bataba ^a, Runling Wang ^c, Cheng Luo ^d, Binghe Wang ^a, Keqin Kathy Li ^{a,b,*}, Peng George Wang ^{a,**}

^a Chemistry Department and Center for Diagnostics and Therapeutics, Georgia State University, Atlanta, GA 30303, USA

^b State Key Laboratory of Medical Genomics, Shanghai Jiao Tong University, Shanghai, China

^c Tianjin Key Laboratory on Technologies Enabling Development of Clinical Therapeutics and Diagnostics (Theranostics), School of Pharmacy, Tianjin Medical University, Tianjin 300070, China

^d Drug Discovery and Design Center, State Key Laboratory of Drug Research, Shanghai Institute of Materia Medica, Chinese Academy of Sciences, Shanghai, China

ARTICLE INFO

Article history:

Received 3 February 2016

Received in revised form

13 June 2016

Accepted 15 June 2016

Available online 21 June 2016

Keywords:

Lysine methyltransferase

G9a inhibitor

Leukemia

MALDI-TOF assay

InChIKey:

PMPKMTDYPOAEEH-UHFFFAOYSA-N

ABSTRACT

Lysine methyltransferase G9a regulates the transcription of multiple genes by primarily catalyzing mono- and di-methylation of histone H3 lysine 9, as well as several non-histone lysine sites. An attractive therapeutic target in treating leukemia, knockout studies of G9a in mice have found dramatically slowed proliferation and self-renewal of acute myeloid leukemia (AML) cells due to the attenuation of HoxA9-dependent transcription. In this study, a series of compounds were identified as potential inhibitors through structure-based virtual screening. Among these compounds, a new G9a inhibitor, DCG066, was confirmed by *in vitro* biochemical, and cell based enzyme assays. DCG066 has a novel molecular scaffold unlike other G9a inhibitors presently available. Similar to G9a's histone substrate, DCG066 can bind directly to G9a and inhibit methyltransferase activity *in vitro*. In addition to suppressing G9a methyltransferase activity and reducing histone H3 methylation levels, DCG066 displays low cytotoxicity in leukemia cell lines with high levels of G9a expression, including K562. This work presents DCG066 as an inhibitor of G9a with a novel structure, providing both a lead in G9a inhibitor design and a means for probing the functionality of G9a.

© 2016 Elsevier Masson SAS. All rights reserved.

1. Introduction

Epigenetic regulation plays a vital role in gene transcription and expression, occurring not through alterations in the genetic code, but rather by modifications to histones or other vital proteins. Among the regulatory processes utilized in posttranslational modifications, histone modification is crucial [1]. Comprised of at least eight variations, including acetylation, methylation, phosphorylation, sumoylation and so forth, the causal relation between histone methylation in gene expression and histone lysine residues

is unusual [2]. Frequently, the methylation of H4 lysine 20 (H4K20), H3 lysine 9 (H3K9), and H3 lysine 27 (H3K27) are associated with transcription suppression, whereas methylation of H3 lysine 4 (H3K4), H3 lysine 36 (H3K36) and H3 lysine 79 (H3K79) tends lead to transcription activation [2–8]. Of interest, H3K9-methylation correlates with transcription suppression, gene silencing and genomic stability. H3K9-methylation is regulated by histone lysine N-methyltransferase EHMT2 (G9a) and analogous protein GLP (G9a like protein). G9a is responsible for catalyzing the mono- and di-methylation of H3K9 in euchromatic regions. G9a is also capable of methylating H3K27, lysine 373 of p53 and other gene expression regulators. However in several cancers, particularly chronic myeloid leukemia, G9a and homologous protein GLP are found to be overexpressed with the proliferation of cancer cells suppressed through knocking out G9a [9,10]. Because G9a and GLP also play a significant role in gametogenesis and embryonic development [11–14], G9a/GLP inhibitors have been used with success in cell

* Corresponding author. Chemistry Department and Center for Diagnostics and Therapeutics, Georgia State University, Atlanta, GA 30303, USA.

** Corresponding author.

E-mail addresses: kli10@gsu.edu (K.K. Li), pwang11@gsu.edu (P.G. Wang).

¹ These authors contributed equally.

reprogramming studies and in producing inducible pluripotent stem cells (iPSCs) by various groups [15–18]. As displayed in Table 1, current G9a inhibitors can be classified into three overall categories: type I with BIX-01294 and its derivatives [19,20], type II with BIX-0138 and its derivatives [21], and type III with fungal metabolite chaetocin [22,23]. Reported in 2007, BIX-01294 was the first G9a selective inhibitor that did not target the binding pocket of cofactor *S*-adenosyl-methionine (SAM) [24]. Since the discovery of BIX-01294, many G9a inhibitors including UNC0224, UNC0638, UNC0642, E72 and A-366 have emerged based on the pharmacophore of BIX-01294 [19,21,25–28]. All of the current G9a inhibitors possess the same quinazoline core and display similar biological activity, performing well in enzyme and cellular assays.

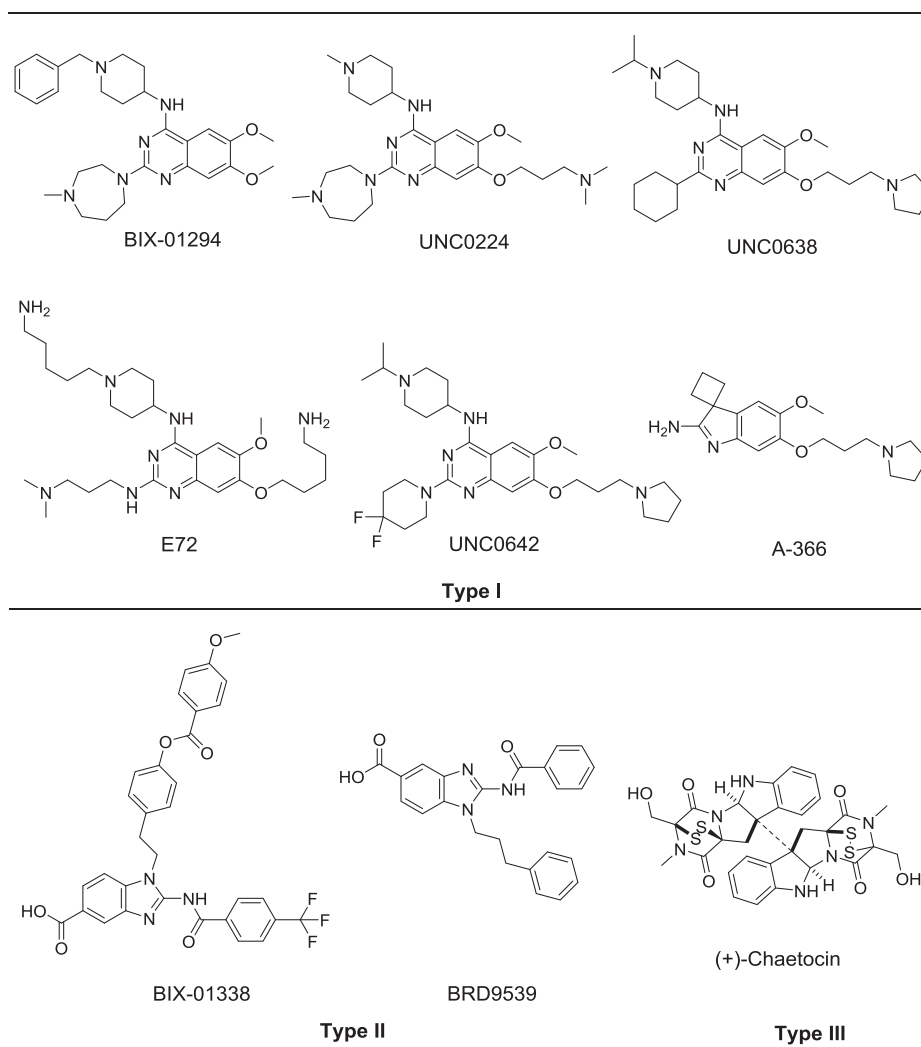
Of particular interest is the inhibitors belonging to the type I and III categories, as clinical trials have indicated their high efficacy in inhibiting the proliferation of leukemia cells. By attenuating HoxA9-dependent transcription, G9a inhibitors are able to reduce the self-renewal and proliferation of acute myeloid leukemia (AML) cells [20]. Previous studies have indicated that mutations involved in DNA methylation could be responsible for mediating abnormal self-renewal and differentiation in leukemia stem cells (LSCs) and, discovery of targeted drugs for epigenetic enzymes could provide a

new route for leukemia treatment [29,30]. G9a has emerged as an attractive drug target for leukemia. However, current inhibitors of G9a are derivatives of parent compound BIX-01294 generated through manual or structure-activity relationship (SAR) analysis, offering limited design space for new inhibitors. Thus there is an interest in searching for new scaffolds capable of inhibiting its activity. This study aims to search for new scaffolds for G9a inhibition through a combination of virtual and enzymatic screening.

High-throughput and structure-based virtual screenings (SBVS) are widely utilized methods in the discovery of lead structures. Through SBVS, DCG066 was identified as an inhibitor with binding affinity comparable to that of the native substrates. *In vitro* biochemical and cell based assays verified that DCG066 had a level of activity comparable to that of BIX-01294, in addition to induction of cell apoptosis. In studying inhibitors for G9a, the expression levels of G9a in varying cancer cell lines were also examined to determine which cell line would be most appropriate for *in vitro* assays. From these observations, a trend emerged; the expression levels of G9a in most hematologic cancer cells were much higher than in normal blood cells.

Since the overexpression of G9a is related to several cancers [31], we analyzed the G9a mRNA and protein level using

Table 1
Structures of known G9a inhibitors.



quantitative real-time PCR and western blotting, respectively, in order to quantify expression levels across different cell lines. K562, a leukemia cell line, was found to have G9a expression levels higher than all solid tumor cells, and thus was used in further *in vitro* cell assays. DCG066 decreases di-methylation levels of histone H3 lysine 9 (H3K9Me2), inhibits cell proliferation and induces cell apoptosis. Displaying comparable activity to BIX-01294 and lower cytotoxicity in leukemia cells, DCG066 offers possibilities as both a probe for the functions of G9a and as a novel lead in G9a inhibitor design.

2. Results and discussion

2.1. Virtual screening

A schematic representation of the overall procedure is presented in Fig. 1. The crystal structure of G9a in complex with UNCO638 (PDB entry: 3RJW) was selected to be the binding pocket in docking studies. Chain A of the protein and the corresponding UNCO683 were both extracted from 3RJW to serve as the template for the binding pocket model. In generating the library of compounds to screen, we searched for a public database containing a large number of small molecule compounds that would be available for subsequent *in vitro* screening. The SPECS database (<http://www.specs.net/>), containing 200,000 small molecule compounds, was found to meet the criteria. The database was then filtered for compounds with log P value smaller than 5 by Pipeline Pilot 7.5, leaving about 90,000 compounds that would likely be soluble in aqueous solution to a certain degree. In evaluating which of the two available docking methods (Glide 5.5, Gold 5.0) were to be used, two criteria were employed: the root mean-square deviation (RMSD) value and the enrichment factor. The RMSD value of UNCO683 between the best-ranked pose by the docking methods and the initial pose would provide a measure for the accuracy of the docking algorithm in comparison with experimentally determined results. The enrichment factor would measure the fraction of active compounds found in a certain percentage divided by the fraction of the screened library. Between these two criteria, Glide 5.5 was found to be the best and was used in docking studies. The Glide XP mode with default settings was used, following standard procedure. The hit compounds were ranked based on G-score and the top 1000 compounds were selected for scaffold diversity analysis by Pipeline Pilot 7.5 and visual inspection. Afterwards, candidate molecules were chosen based on the following criteria: (1) molecular weight of the ligand is lower than 600 Da, which would benefit from further structural optimization, (2) both geometric and chemical features correspond with the active site of G9a, and (3) the binding poses and chemical structures were reasonable. From this, 125 candidate molecules were identified for purchase and further G9a inhibition activity assessment.

2.2. *In vitro* screening for direct binding and enzymatic inhibition

To verify whether the 125 selected compounds could inhibit G9a activity, two different approaches were used to determine the direct binding and the enzymatic inhibition. Surface plasmon resonance (SPR) biosensor (Biacore 3000) was used to test for binding affinity; this was followed by radioactive methylation assay to test the inhibition of enzymatic activity.

As SPR is one of the best methods for studying label-free binding affinity [32,33], it is frequently used in drug discovery. To verify whether the 125 compounds could potentially inhibit G9a activity through direct binding to the enzyme, we carried out the experiments by using Biacore 3000. G9a was immobilized on the sensor chip; then the ligand and the candidate compounds sequentially

flowed over the chip surface in the concentration range of 10–100 μ M. Any interactions between the compounds and G9a would be detected as changes of response units (RU) in the sensorgram. Among the 125 candidates, 14 were found to interact with G9a (Fig. S1A). The sensorgram response to the candidate compounds ranged from 10RU to approximately 200RU. Compounds that failed to display any interactions with G9a were excluded from subsequent testing.

Having recognized that 14 of the compounds screened showed significant binding with G9a, we employed a tritium (H^3)-labeled radioactive methylation assay to test the inhibition of enzymatic activity [34]. 10 μ M solutions of the compounds were used for radioactive assays and four of these compounds displayed more than 50% inhibition at this concentration. Of these four compounds, DCG066 displayed inhibition comparable to that of BIX-01294 (Table 2). As indicated in Table 2, all four compounds possess molecular structures that do not fall into any of the three categories of existing G9a inhibitors. In an enzyme inhibition assay, DCG066 also displayed similar activity as BIX-01294 (Fig. 2A and B). Tentatively, the newly discovered DCG066 could be classified as a type IV inhibitor.

2.3. Chemistry

For confirmation and further detailed mechanistic studies, we synthesized DCG066 (Scheme 1). Commercially available methyl 1-benzylpiperidine-4-carboxylate (**1**) was used as the starting material to synthesize **3** upon reaction with 1-bromo-4-(trifluoromethyl)benzene (**2**) after lithiation. Subsequent hydrogenolysis afforded a free secondary amine (**4**), which was converted to **6** upon nucleophilic substitution with *para*-nitrobenzylchloride (**5**). Reduction of the nitro group to amine **7** followed by reaction with dimethylcarbamic chloride yielded the targeted compound DCG066.

2.4. MALDI-TOF mass spectrum-based biochemical assay

To confirm the result of the radioactive methylation assay, MALDI-TOF mass spectrum was used to quantitatively determine the methylation of the histone H3 peptides catalyzed by G9a enzyme with and without DCG066. 100 nM of protein G9a, 2 μ M of substrate peptide and 1 μ M S-adenosyl methionine (SAM) were added to 50 mM HEPES pH 8.0, 5 μ g/mL BSA and 0.1% β -mercaptoethanol with DCG066 at a final concentration of 10 μ M. After 30 min of reaction, TFA was added to the buffer to terminate the reaction. 1 μ L of the reaction solution was used to detect the modifications of histone H3 (1–24). The relative intensity of H3K9me2 in the sample after the addition of DCG066 was found to be lower than that without DCG066, indicating the ability for DCG066 to inhibit H3K9-dimethylation (Fig. 2C and D).

2.5. DCG066 inhibits cancer cell proliferation, decreases histone H3 lysine 9 (H3K9) di-methyl levels, blocks cell cycle and induces apoptosis

In order to find a good system to test the G9a inhibitor's inhibition activity in cell, the distinction of G9a gene expression between cancer tissues and normal tissue were analyzed by using GENT [35,36] (*Gene Expression across Normal and Tumor tissues*) database (<http://medical-genome.kribb.re.kr/GENT/>). Meanwhile, the G9a gene expression levels of all available cancer cell lines were analyzed by using the databased of *Broad-Novartis Cancer Cell Line Encyclopedia* (<http://www.broadinstitute.org/ccle/home>). Compared to normal cells, G9a expression levels of cancer cells are higher, especially in malignant hematologic cancer cell lines

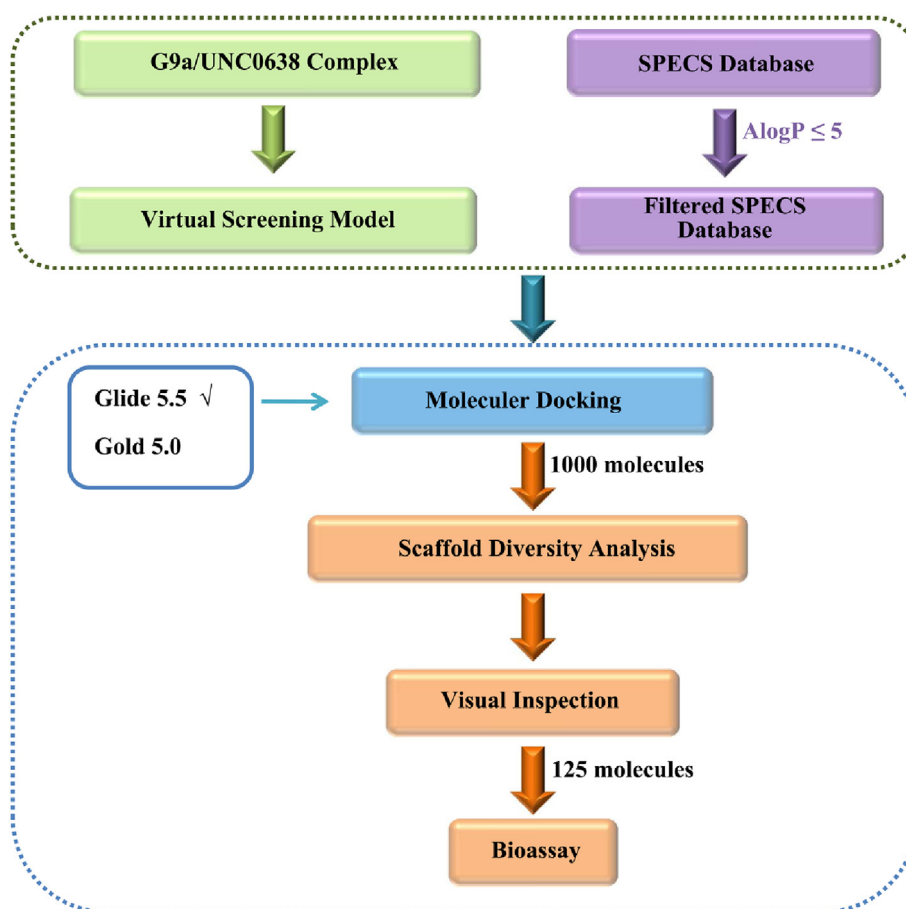


Fig. 1. Flowchart of small molecule virtual screening.

(Fig. 3A and B). To ensure that the cell lines used in our following experiments have appropriate levels of G9a expressed, the G9a mRNA expression levels were tested by using real time-PCR (Fig. 3C) and G9a protein expression levels were checked by using western blot (Fig. 3D). mRNA and protein levels of G9a in the tested leukemia cells (HL60 and K562 cell lines) are higher than the levels in solid cancer cells (A549 for lung cancer and HepG2 for liver cancer). Although normal cells (HUVEC) has detectable G9a protein expressed, it is obviously lower than that in leukemia cells.

Throughout the *in vitro* enzymatic activity assay, DCG066 is the best compound in inhibiting G9a activity among the 125 tested compounds. To verify the ability of these compounds to inhibit cell proliferation, DCG066 was tested at varying concentrations in HL60, K562, A549 and HepG2 cell lines, and BIX-01294 was used as a control (Fig. 4A). The half maximal inhibitory concentrations (IC_{50}) of DCG066 were roughly equivalent to BIX-01294 across the cell lines, with K562 displaying the greatest sensitivity to DCG066 ($IC_{50} = 1.7 \pm 0.3 \mu\text{M}$) (supplement Fig. S3 A).

DCG066 was also considered for its ability to decrease the level of dimethylated histone substrate (H3K9me2). After treating K562 cells with DCG066 at varying concentrations (0.5 μM –2 μM) and incubating for 72 h, histones were extracted from cell. The quantified total histones were measured through immuno-blotting by using anti-histone H3 antibody (Cell Signaling Technology) and anti-histone H3 methylation antibodies (Abcam) to detect expression levels of the relevant histone methylation levels. DCG066 reduced histone H3 lysine 9 dimethylation (H3K9Me2) levels in a similar manner as BIX-01294 (Fig. 4B). 1.0–2.0 μM DCG066 decreased H3K9-dimethylation in K562 cells, but displayed no

changes in H3K27 tri-methylation (supplement Fig. S3 B). Based on these findings, it can be concluded that DCG066 is a G9a selective inhibitor.

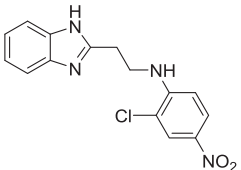
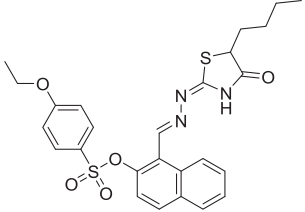
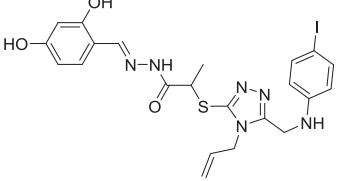
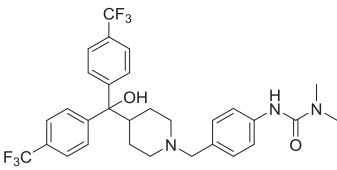
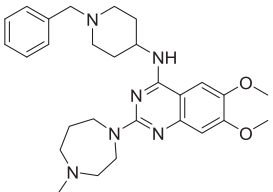
Upon confirming DCG066's ability to inhibit K562 cell proliferation, the potential impact of DCG066 on the cell cycle and apoptosis was investigated. After treating K562 cells with DCG066 and incubating for 24 h, cell cycle and apoptosis were detected using flow cytometry. DCG066 was found to block the cell cycle at stage G2/M in the K562 cells, potentially leading to cell apoptosis (Fig. 4D, C).

2.6. DCG066 binding pocket similarity to BIX-01294 binding pocket

To examine the interactions between DCG066 and G9a, a kinetic assay by SPR was used with concentrations of DCG066 ranging from 25 μM to 300 μM . The test was performed using Biacore 3000 in Wizard mode (Fig. 2D). To calculate the affinity constant, a steady state affinity model was used ($K_d = 18.05 \pm 2.48 \mu\text{M}$).

To better understand the binding mechanism, we conducted molecular docking studies with the two positive controls (UNC0638 and BIX-01294) and the selected 14 molecules from virtual screening. Because UNC0638 is also the co-crystallized ligand, we calculated RMSD between the re-docked ligand and co-crystallized ligand. Our result showed that the RMSD value is 0.995 Å, suggesting our re-docking procedure is reliable. All 16 re-docked molecules are ranked by "Docking Score" and "Enzymatic Inhibit Activity" (supplementary S1B). Considering the overall ranking, DCG066 has the highest performance, therefore DCG066 was chosen for the detailed study (supplementary S1B). Selected

Table 2
Chemical structures of identified small molecules and their inhibition potency.

(Tentative type IV)				
Hypo-thesis	SPECS ID	Compound structure	Inhibition ratio ^a %	Cell inhibition ^a %
DCG001	AH-034/32473019		61	34
DCG020	AE-848/11486036		74	65
DCG033	AK-968/40335567		74	91
DCG066	AK-105/40833871		98	97
BIX-01294	–		88	98

^a Compounds used in both G9a enzyme inhibition assay and cell proliferation inhibition assay had a concentration of 10 μ M.

docking result images were rendered in supplementary S1C. We also studied the interactions between DCG066 and G9a compared to BIX-01294 and UNCO638 (Fig. 5). Top scored conformations were chosen for analysis. Results indicated that UNCO638, BIX-01294 and DCG066 all bind to the peptide substrate pocket (Fig. 5A and B). From the model, BIX and DCG066 were shown to form hydrophobic contacts with residues Y1085, Y1067, F1087, F1152, Y1154, R1157 and F1158 (Fig. 5C–F). In addition to these, DCG066 also forms extra hydrogen bonds with Y1154 and R1157 (Fig. 5F), offering a potential explanation of its binding.

3. Conclusion

H3K9 methylation is a crucial epigenetic regulator in gene transcription and embryonic cell differentiation. Thus, G9a is emerging as a drug target for leukemia treatments. Recent studies have shown that G9a may selectively regulate the fast proliferating myeloid progenitors, but displays no effects on hematopoietic stem cells (HSCs). Primary acute myeloid leukemia (AML) cells from patients are found to be sensitive to G9a inhibition, causing reduction in proliferation and self-renewal through attenuating

HoxA9-dependent transcription [20].

Many of the current G9a selective inhibitors can be sorted into three categories, all of which are derivatives of BIX-01294. In this study, a number of small molecules from the SPECS Database were screened using virtual screening to discover potential G9a inhibitors. Virtual screening followed by bioassays allowed us to identify a new scaffold embedded in DCG066 for further inhibitor development. Initially we investigated various cancer cell lines for their G9a expression profile using immune assay, and found leukemia cell lines to have the highest expression levels of target protein, hence this cell line were used for the cell based assay. Inhibition of cancer cell growth was tested by CCK8 and the IC₅₀ of DCG066 found to be comparable to BIX-01294 (1.7 ± 0.1 and 3.9 ± 0.3 respectively in K562 cell line). DCG066 also demonstrated the ability to induce apoptosis through blocking the cell cycle at stage G2/M in the K562 cells. Further experiments with DCG066 showed that compound decreased H3K9 dimethylation levels in K562 cells.

To examine the interactions between DCG066 and the catalytic domain of G9a more closely, a binding assay was performed by SPR and the structure-function relationship was modeled using GLIDE.

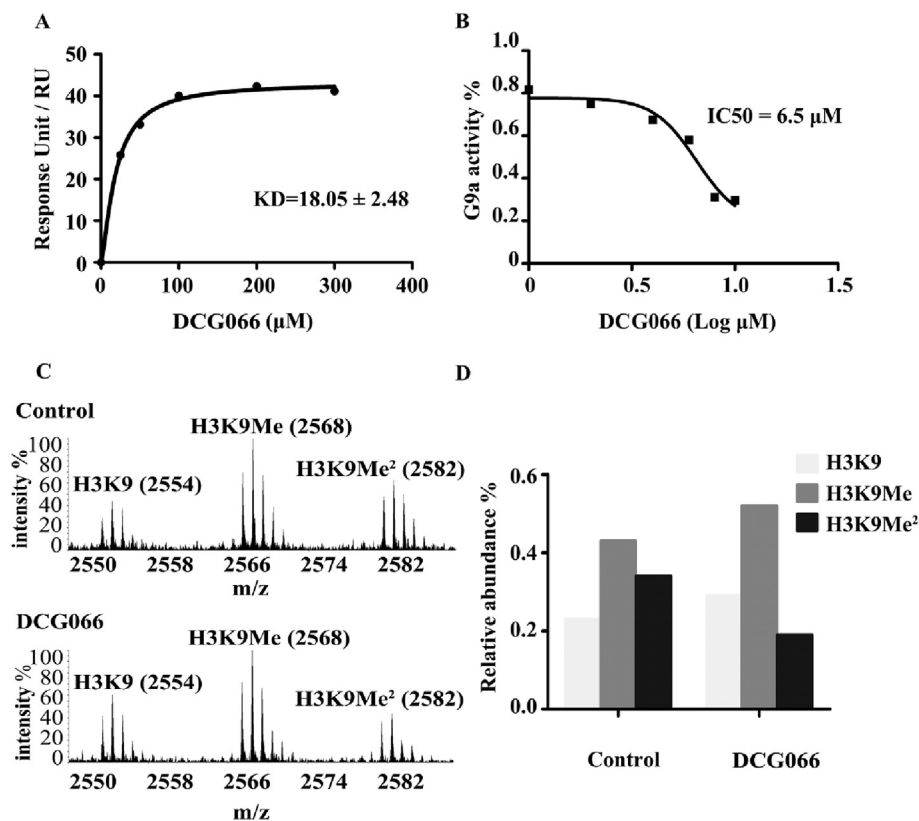
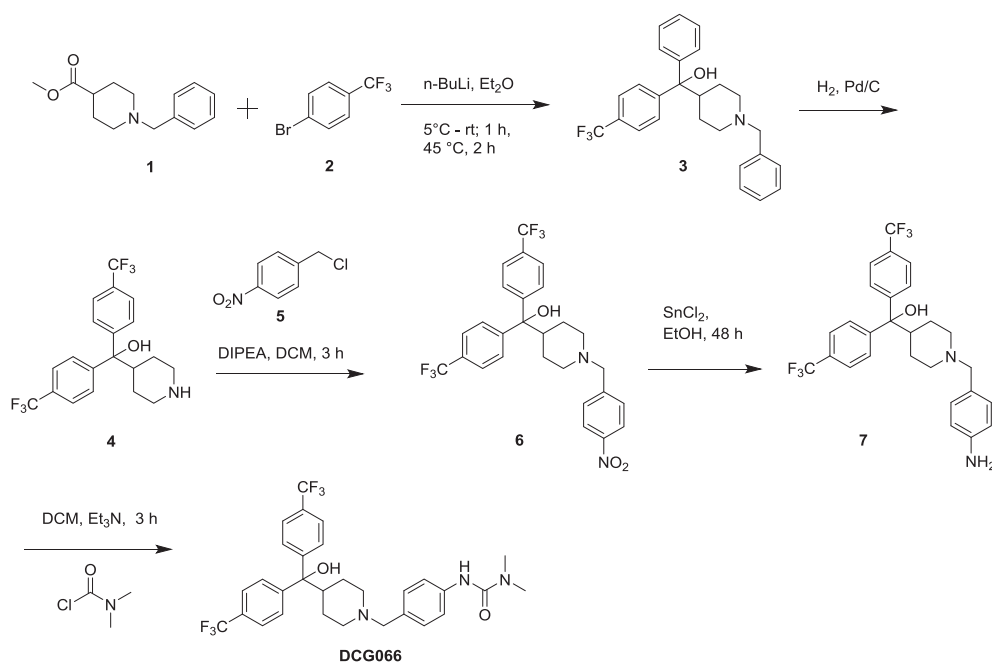


Fig. 2. *In vitro* kinetic assay and enzyme activity inhibition of DCG066. **(A)** Binding assay of DCG066 and recombinant G9a catalytic domain by Biacore 3000. In this assay, G9a protein was immobilized on the CM5 sensor chip as ligand by amine coupling. The concentration of DCG066 was range from 25 μM to 300 μM . Since the sensorgram of each concentration can reach equilibrium, we choose steady-state analysis to calculate the affinity constant (K_d) of DCG066. The K_d is approximately 18 μM calculated by nonlinear least-square (NLSQ) fitting. **(B)** DCG066 can inhibit G9a methyltransferase activity with an IC_{50} of 6.5 μM , which is similar to that of BIX-01294. **(C, D)** In MADI-TOF-MS, dimethyl level of synthetic peptide of histone H3 (1–20) decreased with the addition of DCG066, while the monomethyl level increased.



Scheme 1. Synthesis of DCG066.

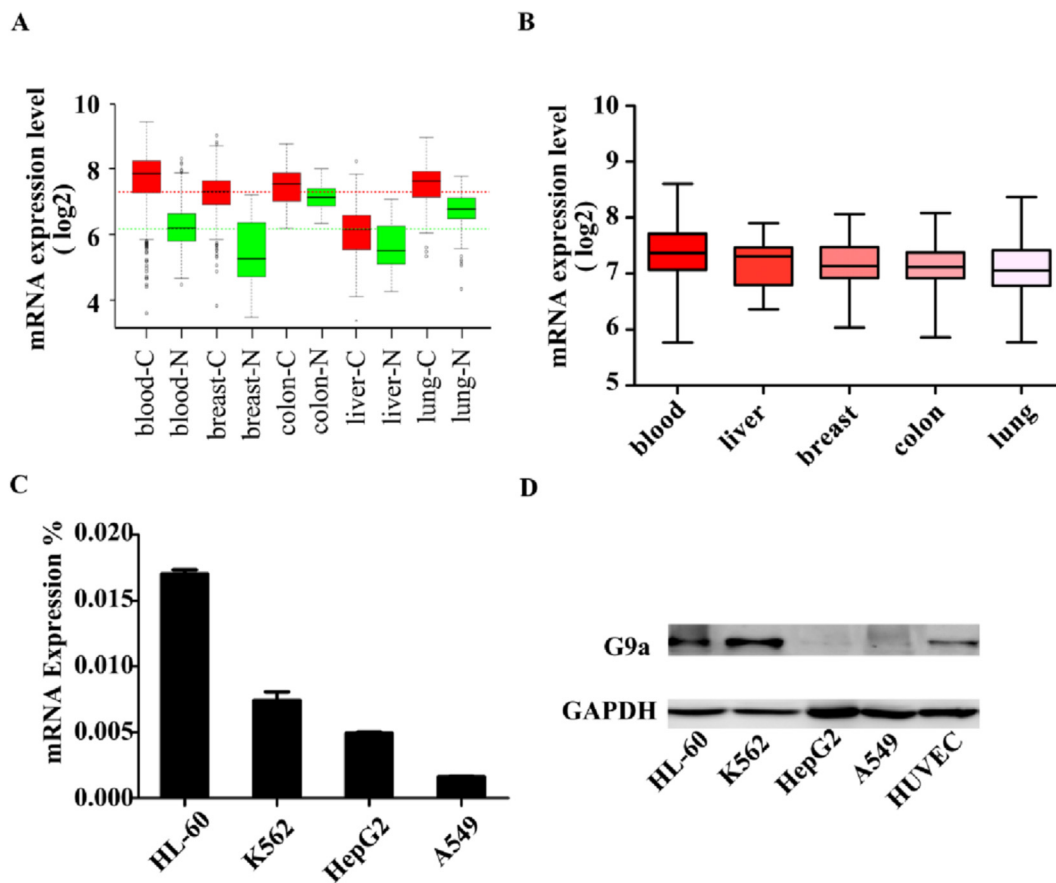


Fig. 3. G9a expression in human tissues and cancer cell lines. (A) Pattern of G9a expression across diverse normal and tumor tissues was obtained from GENT (<http://medical-genome.kribb.re.kr/GENT/>). The average G9a expression in cancer tissue is higher than normal tissues, particularly for hematology system. (B) Analysis of G9a expression level in different cancer cell lines. The statistical data was obtained from CCLE (<http://www.broadinstitute.org/ccle/home>). G9a is expressed higher in leukemia cell lines than other cancer cells. (C, D) The expression of G9a in different cancer cells (K562, HL-60, HepG2, A549 and HUVEC) was detected in both mRNA level (C) and protein level (D). Expression of G9a in leukemia cells is higher than other cancer cells (A549 and HepG2) and normal cells (HUVEC).

DCG066 can bind to G9a with low dissociation constant ($K_d = 18 \mu\text{M}$) as measured by SPR. While DCG066 binds in the peptide substrate pocket in G9a with a pose similar to BIX-01294, DCG066 forms extra hydrogen bonds with residues Y1154 and R1157, suggesting an explanation for the relative activity between the two molecules.

In this study, a new lead compound for G9a inhibition with a similar activity to BIX-01294 and a novel structure, DCG066, was identified from a database of small molecules. This discovery provides both new avenues in G9a inhibitor design and a potential probe for G9a. In future studies, we plan to examine the structure-activity relationship (SAR) of DCG066 analogs to G9a in an effort to improve potency and reduce toxicity.

4. Experimental section

4.1. Materials and physical measurements

All reactions were carried out under an atmosphere of dry nitrogen. All reagents and anhydrous solvents were obtained commercially and used without further purification. ^1H NMR spectra were recorded at 400 MHz and ^{13}C NMR spectra were recorded at 100 MHz using Me_4Si as an internal standard. High-resolution mass spectra (MS) data were acquired using a Thermo-Fisher Orbitrap Elite mass spectrometer with an electrospray ionization (ESI) source. All the samples were run under FT control at

600,000 resolution. All chromatographic purification was performed on Biotage Isolera One using normal phase silica gel 60. HPLC chromatogram for DCG066 compound was acquired using an Agilent 6110 Series system with UV detector set to 254 nm. Samples were injected (5 μL) onto an Agilent Eclipse Plus 4.6 \times 250 mm, 3.5 μM , C18 column at room temperature. Sample was eluted using a linear gradient of 5%–95% B (ACN + 0.1% TFA) in 30 min with A being H_2O + 0.1% TFA. DCG066 had >95% purity using the HPLC method described above.

4.2. Chemistry

4.2.1. (1-Benzylpiperidin-4-yl)bis(4-(trifluoromethyl)phenyl)methanol

Synthesis of the intermediate compound **6** was carried out according to the previously reported procedure [37]. *n*-Butyllithium solution (19 mL, 1.6 M in hexane) was added to 6.8 g of 4-bromobenzotrifluoride **2** (30 mmol) in diethyl ether. To this mixture 2.4 g (10 mmol) of methyl-1-benzylpiperidine-4-carboxylate **1** were added dropwise at 5 $^\circ\text{C}$. The reaction mixture was stirred at room temperature for 1 h and at 45 $^\circ\text{C}$ for 2 h. The crude product was obtained according to the reported procedures, and purified by silica gel flash column chromatography using 0–50% ethyl acetate/hexane as eluent to yield a brown solid. (4.4 g, 77% yield). ^1H NMR (CDCl_3): δ 7.64 (m, 8H, 2 \times trifluoromethylphenyl ArH), 7.33–7.30 (m, 5H, Benzyl ArH) 3.56 (s, 2H, Benzylic CH_2),

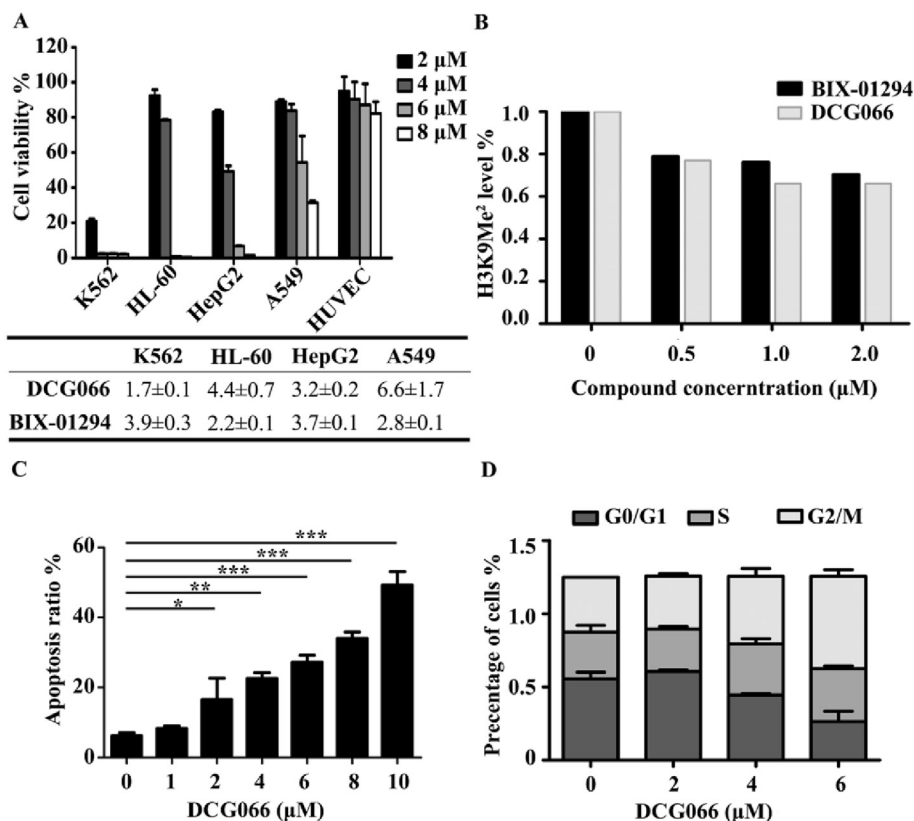


Fig. 4. The anti-cancer effect of DCG066 in cancer cell. (A) DCG066 can inhibit the proliferation of several cancer cells, but effects in healthy cells are small. The cell viability rates shown as bar, the half maximal inhibitory concentrations (IC_{50}) are shown as table under the bar Fig. 4A. The IC_{50} of DCG066 is similar to BIX-01294 and may act better on leukemia cells compared to adherent cells, such as A549 and HepG2. (B) The test of histone methylation level in K562 with the treatment of DCG066. DCG066 can reduce histone H3 lysine 9 dimethylation (H3K9Me₂) levels in a lower concentration than BIX-01294. (C, D) DCG066 can induce apoptosis of K562 cell, with the treatment of 2 μ M DCG066 for 24 h. Meanwhile, DCG066 can block cell cycle in G2/M stage in a low concentration. All these procedures were taken by flow cytometry assay.

3.00–2.97 (m, 2H, N–CH₂–CH₂), 2.54 (t, $J = 11.6$ Hz, 1H, N–CH₂–CH₂–CH), 2.10–2.07 (m, 2H, N–CH₂–CH₂), 1.60–1.45 (m, 4H, 2 \times N–CH₂). ¹³C NMR (CDCl₃) δ 150.9, 149.6, 139.4, 128.4 (2C), 128.1 (4C), 127.3 (2C), 126.1 (2C), 125.8 (2C), 125.3 (3C), 125.2 (2C), 81.4, 62.7, 53.8 (2C), 43.8, 26.2 (2C). HRMS (ESI) m/z : calcd for C₂₇H₂₅F₆NO [M + H]⁺ 494.1919; found 494.1883.

4.2.2. (1-(4-Nitrobenzyl)piperidin-4-yl)bis(4-(trifluoromethyl)phenyl)methanol

The mixture of compound **3** (2 g, 4.04 mmol) and 5 wt% Pd/C (500 mg) in ethanol (200 mL) was stirred for 24 h at room temperature under hydrogen balloon (1 atm). The reaction mixture was filtered and concentrated to a sticky solid. HRMS (ESI) m/z : calcd for C₂₀H₁₉F₆NO [M + H]⁺ 404.1449; found 404.1426. Compound **4** was used for next step without further purification. The mixture of compound **4** (1.2 g, 3 mmol) and DIPEA (1.2 mL) in 10 mL of methylene chloride were added into the solution of 4-nitrobenzylchloride **5** (600 mg, 3.5 mmol) in 20 mL of methylene chloride. The reaction mixture was stirred for 3 h at room temperature; then saturated NaHCO₃ was added. The mixture was extracted with ethyl acetate, washed with water, dried and concentrated to give the crude product, which was purified by column chromatography using 0–40% ethyl acetate/hexane as an eluent to yield a pale yellow solid. (1.1 g; 67% yield). ¹H NMR (CDCl₃): δ 8.17 (d, $J = 8.7$ Hz, 2H, Benzyl, *m*-ArH), 7.61 (m, 8H, 2 \times trifluoromethylphenyl ArH), 7.50 (d, $J = 8.7$ Hz, 2H, Benzyl, *o*-ArH), 3.60 (s, 2H, Benzylic CH₂), 2.92 (m, 2H, N–CH₂–CH₂), 2.52 (m,

1H, N–CH₂–CH₂–CH), 2.12–2.09 (m, 2H, N–CH₂–CH₂), 1.59–1.45 (m, 4H, 2 \times N–CH₂). ¹³C NMR (CDCl₃) δ 149.0 (2C), 147.1, 146.3, 129.4 (4C), 129.0, 126.0 (6C), 125.4 (2C), 125.3, 123.5 (2C), 79.3, 62.1, 53.7 (2C), 43.8, 23.2 (2C). HRMS (ESI) m/z : calcd for C₂₇H₂₄F₆N₂O₃ [M + H]⁺ 539.1769; found 539.1737.

4.2.3. (1-(4-Aminobenzyl)piperidin-4-yl)bis(4-(trifluoromethyl)phenyl)methanol

SnCl₂·2H₂O (900 mg, 4.0 mmol) was added into the solution of compound **6** (1.1 g, 2.0 mmol) in EtOH (20 mL) at r.t., a mild exotherm was observed. The resulting yellow solution was stirred for 2 days, and then the solvent was removed *in vacuo*. The residue was made basic with a 2 N NaOH solution and the aqueous layer was extracted with DCM (2 \times 25 mL). The combined organic layers were dried over Na₂SO₄ and then filtered. The solvent was removed *in vacuo* to yield a pale yellow solid (0.65 g, 65% yield), which was used in the next step without further purification [38]. ¹H NMR (CDCl₃) δ 7.59 (m, 8H, 2 \times trifluoromethylphenyl ArH), 7.07 (d, $J = 7.5$ Hz, 2H, benzyl, *m*-ArH), 6.63 (d, $J = 7.5$ Hz, 2H, benzyl, *o*-ArH), 3.62 (s, 1H, OH), 3.45 (s, 2H, benzylic CH₂), 3.27 (s, 2H, NH₂), 2.97 (d, $J = 11.2$ Hz, 2H, N–CH₂–CH₂), 2.49 (t, $J = 11.6$ Hz, 1H, N–CH₂–CH₂–CH), 2.03 (t, $J = 11.4$ Hz, 2H, N–CH₂–CH₂), 1.69–1.50 (m, 2H, N–CH₂), 1.43 (d, $J = 12.6$ Hz, 2H, N–CH₂). ¹³C NMR (CDCl₃) δ 149.4 (2C), 145.6, 130.7 (4C), 129.1, 128.8, 126.7, 126.1 (2C), 125.4 (4C), 125.2 (2C), 114.9 (2C), 79.28, 62.5, 53.1 (2C), 43.8, 25.7 (2C). HRMS (ESI) m/z : calcd for C₂₇H₂₆F₆N₂O [M + H]⁺ 509.1983; found 509.2000.

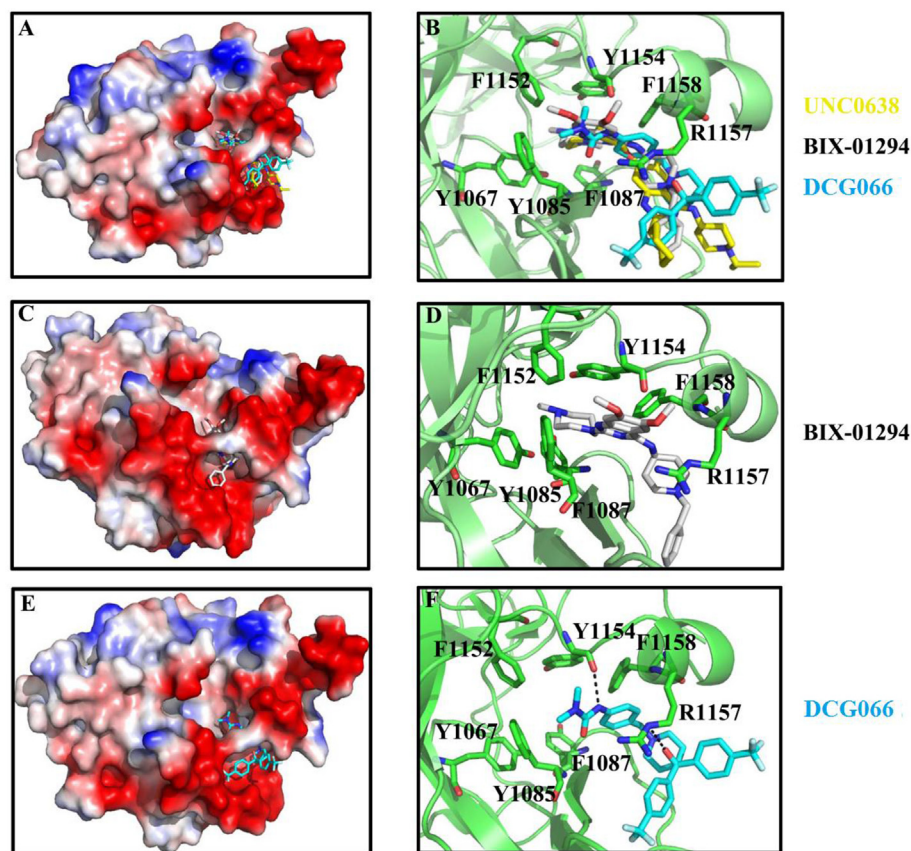


Fig. 5. Complex models of G9a with superimposed inhibitors (UNC0638, BIX-01294, DCG066). Left panel (A, C, E) shows the structural electrostatic surfaces (blue indicates positive charge and red indicates negative charge) and small molecules shows as sticks. Right panel (B, D, F) shows detailed interactions. G9a shows as cartoon in green color and residues, which could form interactions with UNC0638, BIX-01294 or DCG066 are shown as green sticks. (A, B) The binding pocket of crystal structure of G9a-UNC0638 (PDB: 3RJW) [19]. (C, D) The computational model of G9a-BIX-01294. (E, F) The computer mimic model of G9a-DCG066. In these models, the interaction surfaces of all these compounds are very similar. Both BIX-01294 and DCG066 can form hydrophobic interactions with Tyr1085, Tyr1067, Phe1087, Phe1152, Tyr1154, Arg1157 and Phe1158. DCG066 can also form hydrogen bond with Tyr1154 and Arg1157 (F). (For interpretation of the references to color in this figure legend, the reader is referred to the web version of this article.)

4.2.4. 3-(4-((4-(Hydroxybis(4-(trifluoromethyl)phenyl)methyl)piperidin-1-yl)methyl)phenyl)-1,1-dimethylurea (DCG066)

Compound **7** (254 mg, 0.5 mmol) was dissolved in 20 mL of methylene chloride. To this resulting solution was then added DIPEA (0.18 mL, 1 mmol). After stirring for 30 min at 0 °C, dimethyl carbamoyl chloride (54 μ L, 0.6 mmol) was added and the reaction was stirred for another 3 h. Saturated NaHCO₃ solution was added and the mixture was extracted with DCM (3 \times 20 mL). The combined organic phase was dried over Na₂SO₄ and concentrated under reduced pressure. The residue was purified on silica gel column, eluting with 5% MeOH in DCM (containing 0.5% Et₃N) to give a yellow solid (180 mg, 62% yield). ¹H NMR (CDCl₃): δ 7.57 (m, 8H, 2 \times trifluoromethylphenyl ArH), 7.30 (d, J = 8.4 Hz, 2H, benzyl, *m*-ArH), 7.16 (d, J = 8.4 Hz, 2H, benzyl, *o*-ArH), 6.57 (s, 1H, OH), 3.47 (s, 2H, benzylic CH₂), 2.99 (s, 6H, N(CH₃)₂), 2.91 (d, J = 11.4 Hz, 2H, N-CH₂-CH₂), 2.47 (t, J = 11.6 Hz, 1H, N-CH₂-CH₂-CH), 2.03 (t, J = 11.0 Hz, 2H, N-CH₂-CH₂), 1.60–1.52 (m, 2H, N-CH₂), 1.38 (d, J = 12.3 Hz, 2H, N-CH₂). ¹³C NMR (CDCl₃) δ 155.9, 149.5 (2C), 138.2, 129.8 (2C), 128.9, 128.7, 126.2 (5C), 125.4 (2C), 125.2 (2C), 122.7 (2C), 119.9 (2C), 79.2, 62.3, 53.2 (2C), 43.8, 36.4 (2C), 25.8 (2C). HRMS (ESI) m/z : calcd for C₃₀H₃₁F₆N₃O₂ [M + H]⁺ 580.2354; found 580.2373.

4.3. Pharmacophore-based screening and computational model

Pharmacophore models were automatically constructed using

LigandStout for the further screening. The SPECS database was filtered with log S > -4 to construct a database of theoretically soluble compounds (log P < 5). The compounds were then docked into G9a (PDB entry: 3RJW) at the UNC0638 binding pocket using the GLIDE program in standard precision mode [39]. The compounds with the highest binding characteristics were then purchased from SPECS Corp (The Netherlands). The computer model of compound DCG066 and BIX-01294 were docked into G9a (PDB entry: 3RJW) using GLIDE in the XP mode. The final graphs were drawn by Pymol software. Docking validation of 16 molecules was done using Surflex-Dock 2.1 [40] by following our previous procedures [41]. RMSD value was calculated using Openeye Toolkit [42].

4.4. Biological evaluations

4.4.1. Cloning, protein expression and purification

Mouse histone methyltransferase G9a (969–1263) cDNA was amplified from the cDNA of BALB/c mouse thymus, and the fragment was sub-cloned into a vector with a 6His-sumo tag. The mouse G9a (mG9a) was expressed in *Escherichia coli* BL21 (DE3) by the addition of 1 mM isopropyl-1-thio-D-galactopyranoside (IPTG) and incubated overnight at 16 °C.

The 6His-sumo mG9a (969–1263) protein was purified using the following procedure: harvested cell pellet was re-suspended in 20 mM Tris (pH 8.0), 500 mM NaCl, 0.1% β -mercaptoethanol, and

1 mM PMSF. Cells were lysed by sonicating for 15 s with 6-s intervals for a total of 15 min on an ice bath. The supernatant of cell lysate was loaded onto a Ni²⁺ affinity column (Invitrogen) and eluted with buffer (20 mM Tris-HCl pH 8.0, 500 mM NaCl, 20 mM imidazole, 0.1% β -mercaptoethanol, and 1 mM PMSF). The 6His-sumo tag was cleaved from the column by adding ubiquitin-like-specific protease 1 (ULP-1) at 4 °C for 12 h. Wash buffer was then run through the Ni²⁺ column again and the elution buffer collected. Subsequently, advanced protein purification was done by HiTrap Q HP sequential Superdex 200 10/300 GL. Elute of every step was analyzed by SDS PAGE, stained by Coomassie brilliant blue (CBB).

4.4.2. Tritium-labeled radioactive methylation assay

The tritium labeled radioactive methylation assay was used to test the inhibitory effects of the compounds on enzyme activity [34]. In the methylation assay, 2 μ M biotin labeled peptide substrate, 5 μ M [methyl-³H]-SAM (78 Ci/mmol, PerkinElmer), and varied concentrations of inhibitor were pre-incubated in the reaction buffer (50 mM HEPES pH 8.0, 10 mM NaCl, 1 mM DTT) for 30 min at room temperature. The reaction was initiated by adding recombinant mG9a (969–1263) for a final concentration of 2 μ g/ml. 2 μ L of the reaction mixture was transferred to a 96 well plate coated with avidin (Corning), incubated for 30 min in PBST with 5 mM of unlabeled SAM. The plate was washed 3 times with 200 μ L PBST per well to remove the remaining ³H-SAM. Later, 50 mM HCl was used to elute the avidin binding peptide. Finally the elution buffer mixed with 200 μ L scintillator fluid was analyzed by 1450 Microbeta scintillation counter (PerkinElmer).

4.4.3. MALDI-TOF-MS

The *in vitro* inhibition of G9a by the compounds was measured by MALDI-TOF mass spectrum (4800 Plus MALDI TOF/TOF Analyzer, ABI). 100 nM purified mG9a, 2 μ M synthesized histone H3 (1–24) and 1 μ M non-radioactive S-adenosyl methionine (Sigma) were added into a reaction buffer (50 mM HEPES pH 8.0, 5 μ g/mL BSA and 0.1% β -mercaptoethanol) with or without an inhibitor for a final concentration of 10 μ M. The reaction was incubated at room temperature for an hour, and stopped by TFA addition.

The result of mass spectrum was analyzed using the Data Explorer (TM) software, providing peak area scores while a statistical graph was drawn by Graphpad Prism 5.0.

4.4.4. Surface plasmon resonance

The ability of the small molecular compounds to bind to the target enzyme was tested by using SPR (Biacore 3000, GE). Approximately 5000RU of the target protein was immobilized on a CM5 sensor chip. Test compounds were dissolved in running buffer (PBS + P20 + 5%DMSO) at a concentration of 100 μ M.

To screen the compounds, solutions were sequentially injected for 1 min at the associated stage, dissociated in running buffer for 1 min, and the sensor chip was then regenerated by running buffer for 1 min. In this test, an empty cycle per every 5 cycles was run. From the Biacore evaluation software (BIA evaluation version 4.1), the maximum binding values of every compound were obtained.

For the G9a catalytic domain kinetics assay, five concentrations of the compounds were prepared and DMSO contents in these samples were equivalent with 5%. The test was performed in the Wizard mode; and the injection time and dissociation times were recorded. The results were analyzed using the static analysis option in the BIA evaluation software.

4.4.5. Cell culture

All leukemia cells such as HL-60, K562, U937 and Kasumi-1 were grown in RPMI 1640 with 10% fetal bovine serum (FBS), while adherent cell, including A549, HepG2, HCT116, SW1990, and MDA-

MB-231 were grown in Dulbecco's modified Eagle's medium (DMEM) with 10% FBS.

4.4.6. Human G9a expression level analysis

In this study, G9a expression levels were analyzed both in cancer cell lines and human tissues. CCLE (Cancer Cell Line Encyclopedia, www.broadinstitute.org/ccle/home) and GENT (Gene Expression database of Normal and Tumor tissues, <http://medical-genome.krribb.re.kr/GENT/>) were the databases that provided information regarding gene expression in cancer cell lines and human tissues, respectively.

4.4.7. Quantitative real-time PCR

For quantitative real-time PCR (qRT-PCR), total RNA was extracted and reverse transcribed into cDNA. qRT-PCR was performed in ABI PRISM 7500 using SYBR Green PCR Master mix (Takara). The mRNA expression level of G9a was normalized to the transcript level of GAPDH.

4.4.8. Cell viability analysis

Cell growth inhibition was detected by CCK8 assay (Dojindo). 1×10^4 cell suspensions were dispensed on a 96-well plate, and then pre-incubated for 4 h in a humidified incubator. Compounds were dissolved in DMSO, diluted in DMEM culture medium for a concentration of $10 \times$ stock solution, and added as 10 μ L per well. After incubation for 48 h, 10 μ L of CCK8 solution was added into the wells and the solution was allowed to incubate for 4 h in a CO₂ incubator. Afterwards, the absorbance was measured at 450 nm.

4.4.9. Flow cytometry assays

Cell apoptosis was determined by dual staining with annexin V conjugated to phycoerythrin (PE) and 7-amino-actinomycin (7AAD). K562 cells were treated with 0, 2, 4, 6, 8, 10 μ M of DCG066. After incubation for 24 h, cells were collected and stained with annexin V-PE and 7AAD (BD Pharmingen) for 15 min in the dark and analyzed by flow cytometry. Cells undergoing apoptosis were identified as annexin V⁺ and/or 7AAD⁺ cells.

Additionally, cells (1×10^6) were treated with DCG066 (0, 1, 2, 4 μ M) or DMSO for cell cycle analysis. After 24 h of incubation, cells were collected and washed with cold PBS twice, and then suspended in 300 μ L PBS, fixed by 700 μ L ethanol. The fixed cells were washed by PBS twice and re-suspended in PI/RNase Staining Buffer (BD Pharmingen) and then incubated for 15 min before analysis. Flow cytometry experiments were performed using a LSR II cytometer (BD Pharmingen), and data were analyzed by using the FlowJo 7.6.1 software.

4.4.10. Histone extraction and western blot

Histones from cell lysates were extracted using trichloroacetic acid precipitation as described previously [43]. 1×10^7 cells were harvested by centrifugation at $800 \times g$ for 5 min, and suspended on ice in hypotonic buffer (10 mM Tris-HCl pH 8.0, 1 mM KCl, 1.5 mM MgCl₂, 1 mM DTT, 1 mM PMSF) for 30 min. The cell lysate was centrifuged at $13,000 \times g$ for 10 min, and the supernatant was discarded. The lysate pellets were re-suspended using 0.2 N H₂SO₄, mixing at rotor at 4 °C for 30 min, centrifuged at $13,000 \times g$ for 10 min at 4 °C with the precipitation discarded. 50% trichloroacetic acid (TCA) was added to the supernatant dropwise, and then the resulting solution was centrifuged for 20 min. The pellets were washed twice in ice-cold acetone and then dissolved by adding H₂O. Histone content was quantified by a Bradford assay and purity was tested by Coomassie blue staining.

Extracted histone was denatured by SDS loading buffer. Anti-histone H3 antibody (rabbit), anti-histone H3 lysine 9 trimethyl antibody (mouse), anti-histone H3 lysine 9 trimethyl antibody

(rabbit), and mono- and di-methyl arginine antibody (mouse) were purchased from Abcam. Anti-histone H3 lysine 27 trimethyl antibody (rabbit) was purchased from Millipore.

Acknowledgements

This work was supported by the National Natural Science Foundation of China grants (81270622) to KLI, the China 973 Program (2013CB733700 and 2011CB510102) to KLI and Georgia Research Alliance funding to P.G. Wang.

Appendix A. Supplementary data

Supplementary data associated with this article can be found in the online version, at <http://dx.doi.org/10.1016/j.ejmech.2016.06.028>. These data include MOL files and InChIKeys of the most important compounds described in this article.

References

- [1] T. Kouzarides, Chromatin modifications and their function, *Cell* 128 (2007) 693–705.
- [2] A. Barski, S. Cuddapah, K. Cui, T.Y. Roh, D.E. Schones, Z. Wang, G. Wei, I. Chepelev, K. Zhao, High-resolution profiling of histone methylations in the human genome, *Cell* 129 (2007) 823–837.
- [3] R. Cao, L. Wang, H. Wang, L. Xia, H. Erdjument-Bromage, P. Tempst, R.S. Jones, Y. Zhang, Role of histone H3 lysine 27 methylation in Polycomb-group silencing, *Science* 298 (2002) 1039–1043.
- [4] A. Kirmizis, S.M. Bartley, A. Kuzmichev, R. Margueron, D. Reinberg, R. Green, P.J. Farnham, Silencing of human polycomb target genes is associated with methylation of histone H3 Lys 27, *Genes & Dev.* 18 (2004) 1592–1605.
- [5] G. Schotta, M. Lachner, K. Sarma, A. Ebert, R. Sengupta, G. Reuter, D. Reinberg, T. Jenuwein, A silencing pathway to induce H3-K9 and H4-K20 trimethylation at constitutive heterochromatin, *Genes & Dev.* 18 (2004) 1251–1262.
- [6] A. Shilatifard, Molecular implementation and physiological roles for histone H3 lysine 4 (H3K4) methylation, *Curr. Opin. Cell Biol.* 20 (2008) 341–348.
- [7] A.J. Ruthenburg, C.D. Allis, J. Wysocka, Methylation of lysine 4 on histone H3: intricacy of writing and reading a single epigenetic mark, *Mol. Cell* 25 (2007) 15–30.
- [8] A.G. Evertts, A.L. Manning, X. Wang, N.J. Dyson, B.A. Garcia, H.A. Collier, H4K20 methylation regulates quiescence and chromatin compaction, *Mol. Biol. Cell* 24 (2013) 3025–3037.
- [9] J. Huang, J. Dorsey, S. Chuikov, L. Perez-Burgos, X. Zhang, T. Jenuwein, D. Reinberg, S.L. Berger, G9a and Glp methylate lysine 373 in the tumor suppressor p53, *J. Biol. Chem.* 285 (2010) 9636–9641.
- [10] M.W. Chen, K.T. Hua, H.J. Kao, C.C. Chi, L.H. Wei, G. Johansson, S.G. Shiah, P.S. Chen, Y.M. Jeng, T.Y. Cheng, T.C. Lai, J.S. Chang, Y.H. Jan, M.H. Chien, C.J. Yang, M.S. Huang, M. Hsiao, M.L. Kuo, H3K9 histone methyltransferase G9a promotes lung cancer invasion and metastasis by silencing the cell adhesion molecule Ep-CAM, *Cancer Res.* 70 (2010) 7830–7840.
- [11] V. Russo, N. Bernabo, O. Di Giacinto, A. Martelli, A. Mauro, P. Berardinelli, V. Curini, D. Nardinocchi, M. Mattioli, B. Barboni, H3K9 trimethylation precedes DNA methylation during sheep oogenesis: HDAC1, SUV39H1, G9a, HP1, and DNMTs are involved in these epigenetic events, *J. Histochem. Cytochem. Off. J. Histochem. Soc.* 61 (2013) 75–89.
- [12] N. Feldman, A. Gerson, J. Fang, E. Li, Y. Zhang, Y. Shinkai, H. Cedar, Y. Bergman, G9a-mediated irreversible epigenetic inactivation of Oct-3/4 during early embryogenesis, *Nat. Cell Biol.* 8 (2006) 188–194.
- [13] S. Epsztejn-Litman, N. Feldman, M. Abu-Remaileh, Y. Shufaro, A. Gerson, J. Ueda, R. Deplu, F. Fuks, Y. Shinkai, H. Cedar, Y. Bergman, De novo DNA methylation promoted by G9a prevents reprogramming of embryonically silenced genes, *Nat. Struct. Mol. Biol.* 15 (2008) 1176–1183.
- [14] Y. Ushijima, Y.H. Inoue, T. Konishi, D. Kitazawa, H. Yoshida, K. Shimaji, H. Kimura, M. Yamaguchi, Roles of histone H3K9 methyltransferases during *Drosophila* spermatogenesis, *Chromosome Res. Int. J. Mol. Supramol. Evol. Asp. chromosome Biol.* 20 (2012) 319–331.
- [15] Y. Shi, C. Despons, J.T. Do, H.S. Hahm, H.R. Scholer, S. Ding, Induction of pluripotent stem cells from mouse embryonic fibroblasts by Oct4 and Klf4 with small-molecule compounds, *Cell Stem Cell* 3 (2008) 568–574.
- [16] Y. Shi, J.T. Do, C. Despons, H.S. Hahm, H.R. Scholer, S. Ding, A combined chemical and genetic approach for the generation of induced pluripotent stem cells, *Cell Stem Cell* 2 (2008) 525–528.
- [17] N.V. Mezentseva, J. Yang, K. Kaur, G. Iaffaldano, M.C. Remond, C.A. Eisenberg, L.M. Eisenberg, The histone methyltransferase inhibitor BIX01294 enhances the cardiac potential of bone marrow cells, *Stem Cells Dev.* 22 (2013) 654–667.
- [18] B. Feng, J.-H. Ng, J.-C.D. Heng, H.-H. Ng, Molecules that promote or enhance reprogramming of somatic cells to induced pluripotent stem cells, *Cell Stem Cell* 4 (2009) 301–312.
- [19] M. Vedadi, D. Barsyte-Lovejoy, F. Liu, S. Rival-Gervier, A. Allali-Hassani, V. Labrie, T.J. Wigle, P.A. Dimaggio, G.A. Wasney, A. Siarheyeva, A. Dong, W. Tempel, S.C. Wang, X. Chen, I. Chau, T.J. Mangano, X.P. Huang, C.D. Simpson, S.G. Pattenden, J.L. Norris, D.B. Kireev, A. Tripathy, A. Edwards, B.L. Roth, W.P. Janzen, B.A. Garcia, A. Petronis, J. Ellis, P.J. Brown, S.V. Frye, C.H. Arrowsmith, J. Jin, A chemical probe selectively inhibits G9a and GLP methyltransferase activity in cells, *Nat. Chem. Biol.* 7 (2011) 566–574.
- [20] B. Lehnertz, C. Pabst, L. Su, M. Miller, F. Liu, L. Yi, R. Zhang, J. Krosch, E. Yung, J. Kirschner, P. Rosten, T.M. Underhill, J. Jin, J. Hebert, G. Sauvageau, R.K. Humphries, F.M. Rossi, The methyltransferase G9a regulates HoxA9-dependent transcription in AML, *Genes & Dev.* 28 (2014) 317–327.
- [21] Y. Yuan, Q. Wang, J. Paulk, S. Kubicek, M.M. Kemp, D.J. Adams, A.F. Shamji, B.K. Wagner, S.L. Schreiber, A small-molecule probe of the histone methyltransferase G9a induces cellular senescence in pancreatic adenocarcinoma, *ACS Chem. Biol.* 7 (2012) 1152–1157.
- [22] E. Iwasa, Y. Hamashima, S. Fujishiro, E. Higuchi, A. Ito, M. Yoshida, M. Sodeoka, Total synthesis of (+)-chaetocin and its analogues: their histone methyltransferase G9a inhibitory activity, *J. Am. Chem. Soc.* 132 (2010) 4078–4079.
- [23] H. Chaib, A. Nebbioso, T. Prebet, R. Castellano, S. Garbit, A. Restouin, N. Vey, L. Altucci, Y. Collette, Anti-leukemia activity of chaetocin via death receptor-dependent apoptosis and dual modulation of the histone methyltransferase SUV39H1, *Leukemia* 26 (2012) 662–674.
- [24] S. Kubicek, R.J. O'Sullivan, E.M. August, E.R. Hickey, Q. Zhang, M.L. Teodoro, S. Rea, K. Mechtler, J.A. Kowalski, C.A. Homon, T.A. Kelly, T. Jenuwein, Reversal of H3K9me2 by a small-molecule inhibitor for the G9a histone methyltransferase, *Mol. Cell* 25 (2007) 473–481.
- [25] F. Liu, X. Chen, A. Allali-Hassani, A.M. Quinn, G.A. Wasney, A. Dong, D. Barsyte, I. Koziarzdzki, G. Senisterra, I. Chau, A. Siarheyeva, D.B. Kireev, A. Jadhav, J.M. Herold, S.V. Frye, C.H. Arrowsmith, P.J. Brown, A. Simeonov, M. Vedadi, J. Jin, Discovery of a 2,4-diamino-7-aminoalkoxyquinazoline as a potent and selective inhibitor of histone lysine methyltransferase G9a, *J. Med. Chem.* 52 (2009) 7950–7953.
- [26] F. Liu, D. Barsyte-Lovejoy, A. Allali-Hassani, Y. He, J.M. Herold, X. Chen, C.M. Yates, S.V. Frye, P.J. Brown, J. Huang, M. Vedadi, C.H. Arrowsmith, J. Jin, Optimization of cellular activity of G9a inhibitors 7-aminoalkoxy-quinazolines, *J. Med. Chem.* 54 (2011) 6139–6150.
- [27] F. Liu, D. Barsyte-Lovejoy, F. Li, Y. Xiong, V. Korboukh, X.P. Huang, A. Allali-Hassani, W.P. Janzen, B.L. Roth, S.V. Frye, C.H. Arrowsmith, Discovery of an in vivo chemical probe of the lysine methyltransferases G9a and GLP, *J. Med. Chem.* 56 (21) (2013) 8931–8942.
- [28] R.F. Sweis, M. Plushchev, P.J. Brown, J. Guo, F. Li, D. Maag, A.M. Petros, N.B. Soni, C. Tse, M. Vedadi, M.R. Michaelides, G.G. Chiang, W.N. Pappano, Discovery and development of potent and selective inhibitors of histone methyltransferase G9a, *ACS Med. Chem. Lett.* (2014), 140110075408001.
- [29] X.-J. Yan, J. Xu, Z.-H. Gu, C.-M. Pan, G. Lu, Y. Shen, J.-Y. Shi, Y.-M. Zhu, L. Tang, X.-W. Zhang, Exome sequencing identifies somatic mutations of DNA methyltransferase gene DNMT3A in acute monocytic leukemia, *Nat. Genet.* 43 (2011) 309–315.
- [30] K.K. Li, L.-F. Luo, Y. Shen, J. Xu, Z. Chen, S.-J. Chen, DNA methyltransferases in hematologic malignancies, in: *Seminars in Hematology*, Elsevier, 2013, pp. 48–60.
- [31] M.B. Kunze, D.W. Wright, N.D. Werbeck, J. Kirkpatrick, P.V. Coveney, D.F. Hansen, Loop interactions and dynamics tune the enzymatic activity of the human histone deacetylase 8, *J. Am. Chem. Soc.* 135 (2013) 17862–17868.
- [32] R. Karlsson, SPR for molecular interaction analysis: a review of emerging application areas, *J. Mol. Recognit. JMR* 17 (2004) 151–161.
- [33] K.A. Jun Matsui, Noriaki Hara, Daisuke Miyoshi, Hidemi Nawafune, Katsuyuki Tamaki, Naoki Sugimoto, SPR sensor chip for detection of small molecules using molecularly imprinted polymer with embedded Gold nanoparticles, *Anal. Chem.* 77 (2005) 4282–4285.
- [34] J. Wang, L. Chen, S.H. Sinha, Z. Liang, H. Chai, S. Muniyan, Y.W. Chou, C. Yang, L. Yan, Y. Feng, K.K. Li, M.F. Lin, H. Jiang, Y.G. Zheng, C. Luo, Pharmacophore-based virtual screening and biological evaluation of small molecule inhibitors for protein arginine methylation, *J. Med. Chem.* 55 (2012) 7978–7987.
- [35] J. Barretina, G. Caponigro, N. Stransky, K. Venkatesan, A.A. Margolin, S. Kim, C.J. Wilson, J. Lehar, G.V. Kryukov, D. Sonkin, A. Reddy, M. Liu, L. Murray, M.F. Berger, J.E. Monahan, P. Morais, J. Meltzer, A. Korejwa, J. Jane-Valbuena, F.A. Mapa, J. Thibault, E. Bric-Furlong, P. Raman, A. Shipway, I.H. Engels, J. Cheng, G.K. Yu, J. Yu, P. Aspesi, M. de Silva, K. Jagtap, M.D. Jones, L. Wang, C. Hatton, E. Palescandolo, S. Gupta, S. Mahan, C. Sougnez, R.C. Onofrio, T. Liefeld, L. MacConaill, W. Winckler, M. Reich, N. Li, J.P. Mesirov, S.B. Gabriel, G. Getz, K. Ardlie, V. Chan, V.E. Myer, B.L. Weber, J. Porter, M. Warmuth, P. Finan, J.L. Harris, M. Meyerson, T.R. Golub, M.P. Morrissey, W.R. Sellers, R. Schlegel, L.A. Garraway, The Cancer Cell Line Encyclopedia enables predictive modelling of anticancer drug sensitivity, *Nature* 483 (2012), 603–607.
- [36] G. Shin, T.-W. Kang, S. Yang, S.-J. Baek, Y.-S. Jeong, S.-Y. Kim, GENT: gene expression database of normal and tumor tissues, *Cancer Inf.* 10 (2011) 149–157.
- [37] S. Farooq, S. Trah, A. Jeanguenat, Derivatives of (1-benzyl-piperidine-4-yl)-diphenyl-methanol and their use as pesticide, in: *Google Patents*, 2003.
- [38] B. Lagu, M. Wächter, Quaternary Salt CCR2 Antagonists, U.S. Patent No. 7,799,824, 21 Sep. 2010.
- [39] R.A. Friesner, J.L. Banks, R.B. Murphy, T.A. Halgren, J.J. Klicic, D.T. Mainz, M.P. Repasky, E.H. Knoll, M. Shelly, J.K. Perry, D.E. Shaw, P. Francis, P.S. Shenkin, Glide: a new approach for rapid, accurate docking and scoring. 1.

- Method and assessment of docking accuracy, *J. Med. Chem.* 47 (2004) 1739–1749.
- [40] A.N. Jain, Surflex-Dock 2.1: robust performance from ligand energetic modeling, ring flexibility, and knowledge-based search, *J. Comput. Aided Mol. Des.* 21 (2007) 281–306.
- [41] T.D. Leng, H.F. Si, J. Li, T. Yang, M. Zhu, B. Wang, R.P. Simon, Z.G. Xiong, Amiloride analogs as ASIC1a inhibitors, *CNS Neurosci. Ther.* 22 (6) (2016 Jun 1) 468–476.
- [42] I. OpenEye Scientific Software, USA, www.eyesopen.com, OEChem, in Santa Fe, NM, 2014.
- [43] A.P. Butler, C.V. Byus, T.J. Slaga, Phosphorylation of histones is stimulated by phorbol esters in quiescent Reuber H35 hepatoma cells, *J. Biol. Chem.* 261 (20) (1986 Jul 15) 9421–9425.